Partitioning of canopy and soil CO_2 fluxes in a pine forest at the dry timberline across a 13-year observation period

Rafat Qubaja [a], Fyodor Tatarinov[a], Eyal Rotenberg[a], and Dan Yakir[a*]

[a] Department of Earth and Planetary Sciences, Weizmann Institute of Science, Rehovot 76100, Israel

**Correspondence:* Dan Yakir; email: dan.yakir@weizmann.ac.il

Abstract

Partitioning carbon fluxes is key to understanding the process underlying ecosystem response to change. This study used soil and canopy fluxes with stable isotopes (^{13}C) and radiocarbon (^{14}C) measurements in an 18 km^2, 50-year-old dry (287 mm mean annual precipitation; non-irrigated) *Pinus halepensis* forest plantation in Israel to partition the net ecosystem's CO_2 flux into gross primary productivity (GPP) and ecosystem respiration (Re) and (with the aid of isotopic measurements) soil respiration flux (Rs) into autotrophic (Rsa), heterotrophic (Rh), and inorganic (Ri) components. On an annual scale, GPP and Re measured 655 and 488 g C m^{-2}, respectively, with a net primary productivity (NPP) of 282 g C m^{-2} and carbon-use efficiency (CUE=NPP/GPP) of 0.43. Rs made up 60% of the Re and comprised 24 ± 4%, 23 ± 4%, and 13 ± 1% from Rsa, Rh, and Ri, respectively. The contribution of root and microbial respiration to Re increased during high productivity periods, and inorganic sources were more significant components when the soil water content was low. Comparing the ratio of the respiration components to Re of our mean 2016 values to those of 2003 (mean for 2001–2006) at the same site indicated a decrease in the autotrophic components (roots, foliage, and wood) by about -13%, and an increase in the heterotrophic component (Rh/Re) by about +18%, with similar trends for soil respiration (Rsa/Rs decreasing by -19% and Rh/Rs increasing by +8%, respectively). The soil respiration sensitivity to temperature (Q_{10}) decreased across the same observation period by 36% and 9% in the wet and dry periods, respectively. Low rates of soil carbon loss combined with relatively high belowground carbon allocation (i.e., 38% of canopy CO_2 uptake) and low sensitivity to temperature help explain the high soil organic carbon accumulation and the relatively high ecosystem CUE of the dry forest.

Keywords: Carbon balance, Soil respiration, Autotrophic, Heterotrophic, Inorganic flux, Temperature response, Semi-arid ecosystem, Pine forest, Canopy cover, Soil chamber

1. Introduction

The annual net storage of carbon in the land biosphere, known as net ecosystem production (NEP), is the balance between carbon uptake during gross primary productivity (GPP) and carbon loss during growth, maintenance respiration by plants (i.e., autotrophic respiration, Ra), and decomposition of litter and soil organic matter (i.e., heterotrophic respiration, Rh; Bonan, 2008). The difference between GPP and Ra expresses the net primary production (NPP) and is the net carbon uptake by plants that can be used for new biomass production. Measurements from a range of ecosystems have shown that total plant respiration can be as large as 50% of GPP (e.g., Etzold et al., 2011) and together with Rh comprises total ecosystem respiration (Re, Re=Ra+Rh). The partitioning of the ecosystem carbon fluxes can therefore be summarized as:

$$\mathrm{GPP} = \mathrm{NPP} + \mathrm{Ra} = \mathrm{NEP} + \mathrm{Rh} + \mathrm{Ra} \quad (1)$$

Earlier campaign-based measurements carried out by Maseyk et al. (2008a) and Grünzweig et al. (2009) in the semi-arid *Pinus halepensis* (Aleppo pine) Yatir forest indicated that GPP at this site was lower than among temperate coniferous forests (1,000–1,900 g C m^{-2} y^{-1}) but within the range estimated for Mediterranean evergreen needle-leaf and boreal coniferous forests (Falge et al., 2002; Flechard et al., 2019b), and had a high carbon-use efficiency of 0.4 (CUE = NPP/GPP; DeLucia et al., 2007). The total flux of CO_2 released from the ecosystem (Re) can be partitioned into aboveground autotrophic respiration (i.e., foliage and sapwood, Rf) and soil CO_2 flux (Rs). Rs, in turn, is a combination of three principal components and can be further partitioned into the components originating from roots or rhizospheres and mycorrhizas (i.e., belowground autotrophic, Rsa), from carbon respired during the decomposition of dead organic matter by soil microorganisms and macrofaunal (heterotrophic respiration, Rh; Bahn et al., 2010; Kuzyakov, 2006), and pedogenic or anthropogenic acidification of soils containing $CaCO_3$ (Ri; Joseph et al., 2019; Kuzyakov, 2006), which is expressed as:

$$\mathrm{Re} = \mathrm{Rs} + \mathrm{Rf} = [\mathrm{Rsa} + \mathrm{Rh} + \mathrm{Ri}] + \mathrm{Rf} \quad (2)$$

Previously published results show that the contribution of Rsa and Rh to Rs ranges from 24 to 65% and from 29 to 74%, respectively, in forest soils in different biomes and ecosystems (Binkley et al., 2006; Chen et al., 2010; Flechard et al., 2019a; Frey et al., 2006; Hogberg et al., 2009; Subke et al., 2011). Some studies reported significant proportions of abiotic contribution to Rs, ranging between 10 and 60% (Martí-Roura et al., 2019; Ramnarine et al., 2012; Joseph et al., 2019). However, most of these experiments were performed in boreal, temperate, or subtropical forests, and there is a general lack of information on water-limited environments, such as dry Mediterranean ecosystems. Using both ^{13}C and CO_2/O_2 ratios also showed that abiotic processes, such as CO_2 storage, transport, and interactions with sediments, can influence Rs measurements at such sites (Angert et al., 2015; Carmi et al., 2013). Furthermore, root-

respired CO_2 can also be dissolved in the xylem water and carried upward with the transpiration stream (Etzold et al., 2013).

Rates of the soil-atmosphere CO_2 flux (Rs) have been altered owing to global climatic change, particularly through changes in soil temperature (Ts) and soil moisture (SWC; Bond-Lamberty and Thomson, 2010; Buchmann, 2000; Carvalhais et al., 2014; Hagedorn et al., 2016; Zhou et al., 2009), which could account for 65–92% of the variability of Rs in a mixed deciduous forest (Peterjohn et al., 1994). Soil moisture impacts on Rs have been observed in arid and Mediterranean ecosystems, where Ts and SWC are negatively correlated (e.g., Grünzweig et al., 2009). CO_2 efflux generally increases with increasing soil temperatures (Frank et al., 2002), which can produce positive feedback on climate warming (Conant et al., 1998), converting the biosphere from a net carbon sink to a carbon source (IPCC-AR5 2014). A range of empirical models have been developed to relate Rs rate and temperature (Balogh et al., 2011; Lellei-Kovács et al., 2011), and the most widely used models rely on the Q_{10} approach (Bond-Lamberty and Thomson, 2010), which quantifies the sensitivity of Rs to temperature and can integrate it with physical processes, such as the rate of O_2 diffusion into and CO_2 diffusion out of soils and the intrinsic temperature dependency of enzymatic processes (Davidson and Janssens, 2006). Soil moisture (SWC) may be of greater importance than temperature in influencing Rs in water-limited ecosystems (Hagedorn et al., 2016; Grünzweig et al., 2009; Shen et al., 2008). In general, the Rs rate increases with the increase of SWC at low levels but decreases at high levels of SWC (Deng et al., 2012; Hui and Luo, 2004; Jiang et al., 2013). Several studies highlight the sensitivity of carbon fluxes in semi-arid Mediterranean ecosystems to the irregular seasonal and interannual distribution of rain events (Poulter et al., 2014; Ross et al., 2012). While Rs is generally constrained by low SWC during summer months, abrupt and large soil CO_2 pulses have been observed after rewetting the dry soil (Matteucci et al., 2015).

The objectives were twofold. First, to obtain detail on partitioning of the carbon fluxes in a semi-arid pine forest to help explain the high productivity and carbon use efficiency recently reported for this ecosystem (Qubaja et al., in press), and provide process-based information to assess the carbon sequestration potential of such a semi-arid afforestation system. Second, to combine this 2016 study with the results of a similar one at the same site in 2003 (mean values for 2001–2006; Grünzweig et al., 2007, 2009) to obtain a long-term perspective across 13 years on soil respiration and its partitioning. We hypothesized that the high carbon use efficiency of the dry forest ecosystem is associated with high belowground carbon allocation and relatively low decomposition rates, and that the long-term trend associated with warming may be suppressed by the dry conditions.

2. Materials and methods

2.1. Site description

The Yatir forest (31°20'49" N; 35°03'07" E, 650 m a.s.l.) is situated in the transition zone between sub-humid and arid Mediterranean climates (Fig. SI-1) on the edge of the Hebron mountain ridge. The ecosystem is a semi-arid pine afforestation established in the 1960s and covering approximately 18 km^2. The average air temperatures for January and July are 10.0 ºC and 25.8 ºC, respectively. Mean annual potential evapotranspiration (ET) is 1,600 mm, and mean annual precipitation is 287 mm. Only winter (December to March) precipitation occurs in this region, creating a distinctive wet season, while summer (June to October) is an extended dry season. There are short transition periods between seasons, with a wetting season (i.e., autumn) and a drying season (i.e., spring). The forest is dominated by Aleppo pine (*Pinus halepensis* Mill.), with smaller proportions of other pine species and cypress and little understory vegetation. Tree density in 2007 was 300 trees ha^{-1}; mean tree height was 10.0 m; diameter at breast height (DBH) was ~15.9 cm; and the leaf area index (LAI) was ~1.5. The native background vegetation was sparse shrubland, which is dominated by the dwarf shrub *Sarcopoterium spinosum* (L.) Spach, with patches of herbaceous annuals and perennials reaching a total vegetation height of 0.30–0.50 m (Grünzweig et al., 2003, 2007). The root density range is 30–80 roots m^{-2} at the upper 0.1 m soil depth, falling to the minimum value (~0 roots m^{-2}) at 0.7 m soil depth (Preisler et al., 2019). Biological soil crust (BSC) is evident in the forest but is less than in the surrounding shrub by ~40% (Gelfand et al., 2012).

The soil at the research site is shallow (20–40 cm), reaching only 0.7–1.0 m; the stoniness fraction for the soil depth (0–1.2 m) is 15–60%, and the rock cover of the surface ranges between 9 and 37%, as recently described in detail (Preisler et al., 2019); the soil is eolian-origin loess with a clay-loam texture (31% sand, 41% silt, and 28% clay; density: 1.65 ± 0.14 g cm^{-3}) overlying chalk and limestone bedrock. Deeper soils (up to 1.5 m) are sporadically located at topographic hollows. While the natural rocky hill slopes in the region are known to create flash floods, the forested plantation reduces runoff dramatically to less than 5% of annual rainfall (Shachnovich et al., 2008). Groundwater is deep (>300 m), reducing the possibility of groundwater recharge due to negative hydraulic conductivity or of water uptake by trees from the groundwater.

2.2. Flux and meteorological measurements

An instrumented eddy covariance tower was erected in the geographical center of Yatir forest, following the EUROFLUX methodology (Aubinet et al., 2000). The system uses a three-dimensional (3D) sonic anemometer (Omnidirectional R3, Gill Instruments, Lymington, UK) and a closed path LI-COR 7000 CO_2/H_2O gas analyzer (LI-COR Inc., Lincoln, NE, USA) to measure the evapotranspiration flux (ET) and net CO_2 flux (NEE). EC flux measurements were used to estimate the annual scale of NEP by integrating

half-hour NEE values. The long-term operation of our EC measurement site (since 2000; see Rotenberg and Yakir, 2010) provides continuous flux and meteorological data with about 80% coverage, which are subjected to U* night-time correction and quality control, and gap filling is based on the extent of the missing data, as recently described in more detail in Tatarinov et al. (2016). A site-specific algorithm was used for flux partitioning into Re and GPP. Daytime ecosystem respiration (Re-d, in μmol m^{-2} s^{-1}) was estimated based on measured night-time values (Re-n; i.e., when the global radiation was <5 W m^{-2}), averaged for the first three half-hours of each night. The daytime respiration for each half-hour was calculated according to Eq. 3 (Maseyk et al., 2008a; Tatarinov et al., 2016):

$$R_{e-d} = R_{e-n}(\alpha_1 \beta_s^{dT_s} + \alpha_2 \beta_w^{dT_a} + \alpha_3 \beta_f^{dT_a}) \quad (3)$$

where βs, βw, and βf are coefficients that correspond to soil, wood, and foliage, respectively; dTs and dTa are soil and air temperature deviations from the values at the beginning of the night; and α1, α2, and α3 are partitioning coefficients fixed at 0.5, 0.1, and 0.4, respectively. The βs, βw, and βf coefficients were calculated as follows: βs values were based on Q_{10} from the Grünzweig et al. (2009) study at the same site; where βs = 2.45 for wet soil (i.e., SWC in the upper 30 cm above 20% vol); βs = 1.18 for dry soil (i.e., SWC in the upper 30 cm equal to or below 20% vol); βf = 3.15–0.036 Ta; and βw = 1.34+0.46 exp (-0.5((DoY–162)/66.1)^2), where DoY is the day of the hydrological year starting from 1 October. Finally, GPP was calculated as GPP = NEE–Re. Negative values of the NEE and GPP indicated that the ecosystem was a CO_2 sink.

Half-hour auxiliary measurements used in this study included photosynthetic activity radiation (PAR mol m^{-2} s^{-1}), vapor pressure deficit (VPD, kPa), wind speed (m s^{-1}), and relative humidity (RH, %), with additional measurements as described elsewhere (Tatarinov et al., 2016). Furthermore, the soil microclimatology half-hour measurements were measured and calculated with soil chamber measurements, using the LI-8150-203 (LI-COR, Lincoln, NE), as described below, namely air temperature (Ta, °C) and relative humidity (RH, %) at 20 cm above the soil surface and soil temperature (Ts, °C) at a 5 cm soil depth using a soil temperature probe, as well as volumetric soil water content (SWC_{0-10}, m^3 m^{-3}) in the upper 10 cm of the soil near the chambers, using the ThetaProbe model ML2x (Delta-T Devices Ltd., Cambridge, UK), which was calibrated to the soil composition based on the manufacturer's equations.

2.3. Soil CO_2 fluxes

Soil CO_2 fluxes (Rs) were measured with automated non-steady-state systems, using 20 cm diameter opaque chambers and a multiplexer to allow for simultaneous control of several chambers (LI -8150, -8100-101, -8100-104; LI-COR, Lincoln, NE). The precision of CO_2 measurements in the chambers' air is ±1.5% of the measurements' range (0–20,000 ppm). The chambers were closed on preinstalled PVC collars

20 cm diameter, allowing for short measurement time (i.e., 2 min), and positioned away from the collars for the rest of the time. Data were collected using a system in which air from the chambers was circulated (2.5 l min^{-1}) through an infrared gas analyzer (IRGA) to record CO_2 (µmol CO_2/mol air) and H_2O (mmol H_2O/mol air) concentrations in the system logger (1 s^{-1}). Gap filling of missing data due to technical problems (i.e., 27 % of the data across the study period between November 2015 and October 2016) was based on the average diurnal cycle of each month.

The rates of soil CO_2 flux, Rs (µmol CO_2 m^{-2} s^{-1}), were calculated from chamber data using a linear fit of change in water-corrected CO_2 mole fraction using Eq. 4 (LiCor Manual, 2015) as follows:

$$R_s = \frac{dC}{dt} \cdot \frac{v\,P}{s\,T_a R} \quad . \tag{4}$$

where dC/dt is the rate of change in the water-corrected CO_2 mole fraction (µmol CO_2 mol^{-1} air s^{-1}), v is the system volume (m^3), P is the chamber pressure (Pa), s is the soil surface area within the collar (m^2), Ta is the chamber air temperature (K), and R is the gas constant (J mol^{-1} K^{-1}). A measurement period of 2 minutes was used, based on preliminary tests to obtain the most linear increase of CO_2 in the chambers with the highest R^2.

Soil CO_2 fluxes in the experimental plot were measured between November 2015 and October 2016 by means of three measurement chambers using 21 collars grouped in seven sites in the forest stand, with three locations (i.e., three collars) per site, based on different distances from the nearest tree (Dt). The collars were inserted 5 cm into the soil. Data were recorded on a half-hour basis (48 daily records). The three chambers were rotated between the seven sites every 1–2 weeks to cover all sites and to assess spatial and temporal variations.

Upscaling of the collar measurements to plot-scale soil CO_2 flux was carried out by grouping collars based on three locations (i.e., under trees [<1 m from nearest tree; UT], in gaps between trees [1–2.3 m; BT], and in open areas [>2.3 m; OA]), with one chamber taking measurements at each location, and estimating the fractional areas (Ø) of the three locations based on mapping the sites according to the distances noted above, as previously done by Raz-Yaseef et al. (2010):

$$Rs = Rs_{OA} * Ø_{OA} + Rs_{BT} * Ø_{BT} + Rs_{UT} * Ø_{UT} \tag{5}$$

$$Ø_{OA} + Ø_{BT} + Ø_{UT} = 1 \tag{6}$$

The annual scale of Rs was derived from the upscaled chamber measurements (Eq. 5) based on daily records (48 half-hourly values) of spatial upscaled Rs.

Estimating the temperature sensitivity of Rs (Q_{10}) was performed as described by Davidson and Janssens (2006) using a first-order exponential equation (see also Xu et al., 2015):

$$Rs = ae^{bTs} \quad (7)$$

where Rs represents the half-hour spatial upscaled time series of soil respiration flux (μmol m^{-2} s^{-1}), Ts (°C) is soil temperature at a 5 cm depth (upscaled spatially and temporally using the same method as for Rs), and a and b are fitted parameters. The b values were used to calculate the Q_{10} value according to the following equation:

$$Q_{10} = e^{10b} \quad (8)$$

2.4. Soil CO_2 flux partitioning

Determination of different sources of soil CO_2 efflux was based on linear mixing models (Lin et al., 1999) to estimate proportions for three main sources (autotrophic, heterotrophic, and abiotic), using isotopic analysis of soil CO_2 profiles and soil incubation data from eight campaigns (January to September) during 2016, according to Equations 9–11. Partitioning of the monthly Rs values into components was done using a 3-endmember triangular model for interpreting the $\delta^{13}C$ and $\Delta^{14}C$ values of CO_2 flux; the 3-endmember triangular corners are the autotrophic (Rsa), heterotrophic (Rh), and abiotic (Ri) sources of Rs. The $\delta^{13}C$ and $\Delta^{14}C$ isotope signatures of monthly Rs locate it inside the triangle (Fig. SI-2):

$$\delta^{13}C_{Rs} = f_{sa} * \delta^{13}C_{sa} + f_h * \delta^{13}C_h + f_i * \delta^{13}C_i \quad (9)$$

$$\Delta^{14}C_{Rs} = f_{sa} * \Delta^{14}C_{sa} + f_h * \Delta^{14}C_h + f_i * \Delta^{14}C_i \quad (10)$$

$$1 = f_{sa} + f_h + f_i \quad (11)$$

where f indicates the fraction of total soil flux (e.g., $f_h=R_h/R_s$), while subscripts sa, h, and i indicate autotrophic, heterotrophic, and inorganic components, respectively. The three-equations system was used to solve the three unknown f fractions of the total soil flux based on empirical estimates of the isotopic endmembers. Additionally, $\delta^{13}C$ and $\Delta^{14}C$ are the stable and radioactive carbon isotopic ratios, where $\delta^{13}C = [([^{13}C/^{12}C]_{sample}/[^{13}C/^{12}C]_{reference})-1]*1000‰$ and the reference is the Vienna international standard (VPDB). Radiocarbon data are expressed as $\Delta^{14}C$ in parts per thousand or per mil (‰), which is the deviation of a sample $^{14}C/^{12}C$ ratio relative to the OxI standard in 1950 (see Taylor et al., 2015), that is, $\Delta^{14}C = [([^{14}C/^{12}C]_{sample}/(0.95*[^{14}C/^{12}C]_{reference}*\exp[(y-1950)/8267]))-1]*1000‰$, where y is the year of sample measurements.

The $\delta^{13}C_{Rs}$ was estimated monthly using the Keeling plot approach (Figs SI-3 and 4; Pataki et al., 2003; Taneva and Gonzalez-Meler, 2011). Soil air was sampled using closed-end stainless steel tubes (6 mm diameter) perforated near the tube bottom at four depths (30, 60, 90, and 120 cm). Samples of soil air were collected in pre-evacuated 150 mL glass flasks with high-vacuum valves, the dead volume in the tubing and flask necks having been purged with soil air using a plastic syringe equipped with a three-way valve.

Note that the Keeling plot approach is based on the 2-endmembers mixing model (see Review of Pataki et al., 2003), which often does not hold in soils because of variations in the $\delta^{13}C$ values of source material with depth (see a recent example in Joseph et al., 2019). However, probably because of the very dry conditions at our study site, no change in $\delta^{13}C$ with depth in the root zone is observed (±0.1‰ across the 35 cm depth profiles; Fig. SI-5), providing an opportunity to avoid this caveat. The soil CO_2 samplings carried out therefore represented predominantly the mixing of atmospheric CO_2 with a single integrated soil source signal, consistent with the Keeling plot approach.

The autotrophic ($\delta^{13}C_{sa}$) endmember was estimated based on incubations during the sampling periods of excised roots, following Carbone et al. (2008). Fine roots (<2 mm diameter) were collected, rinsed with deionized water, and incubated for 3 hours in 10 mL glass flasks connected with Swagelok Ultra-Torr tee fittings to 330 mL glass flasks equipped with Louwers high-vacuum-valves. The flasks were flushed with CO_2-free air at room temperature close to field conditions. The CO_2 was allowed to accumulate to at least 2,000 ppm (~2 h).

The heterotrophic ($\delta^{13}C_h$) endmember was estimated as in Taylor et al. (2015), and, similar to the root-incubation experiment, soil samples from the top 5 cm of the litter layer or 10 cm below the soil surface were collected, and roots were carefully removed to isolate heterotrophic components. Root-free soils were placed in 10 mL glass flasks and allowed to incubate for 24 hours before being transferred to evacuated 330 mL glass flasks. The inorganic source ($\delta^{13}C_i$) endmember was estimated using one gram of dry soil (ground to pass through a 0.5 mm mesh) placed in a 10 mL tube with a septum cap; then, 12 mL of 1M HCl was added to dissolve the carbonate fraction, and the fumigated CO_2 withdrawn from each tube was collected using a 10 mL syringe and injected into a 330 mL evacuated flask for isotopic analysis.

Radiocarbon estimates were based on the work of Carmi et al. (2013) at the same site, adjusted to the measured atmospheric ^{14}C values during the study period (49.5‰; Carmi et al., 2013). The $\Delta^{14}C_{sa}$ and $\Delta^{14}C_h$ endmembers were estimated based on the assumption that they carry the ^{14}C signatures of 4 and 8.5 years, respectively, older than the ^{14}C signature of the atmosphere at the time of sampling, based on mean ages previously estimated (Graven et al., 2012; Levin et al., 2010; Taylor et al., 2015). $\Delta^{14}C_i$ was obtained from Carmi et al. (2013). Monthly values of $\Delta^{14}C_{Rs}$ were obtained using the linear equation of the regression line of the measured $\delta^{13}C$ values of Rsa, Rsh, and Ri and the corresponding estimated $\Delta^{14}C$ values (Fig. SI-2) and monthly $\delta^{13}C$ values of Rs.

2.5. Isotopic analysis

Isotopic analysis followed the methodology described in Hemming et al. (2005). The $\delta^{13}C$ of CO_2 in the air was analyzed using a continuous flow mass spectrometer connected to a 15-flask automatic manifold system. An aliquot of 1.5 mL of air was expanded from each flask into a sampling loop on a 15-position valve (Valco Houston, TX, USA). CO_2 was cryogenically trapped from the air samples using helium as a carrier gas; it was then separated from N_2O with a Carbosieve G (Sigma Aldrich) packed column at 70°C and analyzed on a Europa 20-20 Isotope Ratio Mass Spectrometer (Crewe, UK). $\delta^{13}C$ results were quoted in parts per thousand (‰) relative to the VPDB international standard. The analytical precision was 0.1%. To measure [CO_2], an additional 40.0 mL subsample of air from each flask was expanded into mechanical bellows and then passed through an infrared gas analyzer (LICOR 6262; Lincoln, NE, USA) in an automated system. The precision of these measurements was 0.1 ppm. Flasks filled with calibrated standard air were measured with each batch of 10 sample flasks; five standards were measured per 10 samples for $\delta^{13}C$ analyses and four standards per 10 samples for [CO_2] analyses.

Organic matter samples were dried at 60°C and milled using a Wiley Mill fitted with size 40 mesh, and soil samples were ground in a pestle and mortar. Soils containing carbonates were treated with 1M hydrochloric acid. Between 0.2 and 0.4 mg of each dry sample was weighed into tin capsules (Elemental Microanalysis Ltd., Okehampton, UK), and the $\delta^{13}C$ of each was determined using an elemental analyzer linked to a Micromass Optima IRMS (Manchester, UK). Three replicates of each sample were analyzed, and two samples of a laboratory working standard cellulose were measured for every 12 samples. Four samples of the acetanilide (Elemental Microanalysis Ltd.) international standard were used to calibrate each run, and a correction was applied to account for the influence of a blank cup. The precision was 0.1%.

2.6. Total belowground carbon allocation (TBCA)

TBCA (g C m^{-2} y^{-1}) was calculated following Giardina and Ryan (2002) for the study year (November 2015–October 2016) as follows:

$$TBCA = Rs - Rl + \Delta C_{soil} \quad (12)$$

where R_l is the annual aboveground litter production between November 2014 and October 2015, and ΔC_{soil} is the annual change in belowground total soil organic C. Litter production, not measured during the present study, was estimated based on values obtained by Masyk et al. (2008b) for 2000–2006 (56 g C m^{-2} y^{-1}) and assumed to have increased in the study period (2014–2015) proportionally to the measured increase in leaf area index (LAI; 1.31 to 1.9; i.e., R_l = [(1.9*56)/1.31] = 83 g C m^{-2} y^{-1}). For herbaceous litter production, three plots of 25 m^2 were randomly selected in 2002 and harvested at the end of the growing season, total fresh biomass was weighed, and subsamples were used to determine dry weight and C content. Grünzweig et al. (2007) found that herbaceous litter production was close to the average rainfall for the specific year; this method was adapted in the current study for the period between November 2014

and October 2015. Since aboveground litter (Rl; the sum of tree litter and herbaceous litter production) of a given year was mainly produced during that year but decayed during the following hydrological year, TBCA was on the current year's Rs (2015–2016) and the previous year's Rl (2014–2015). ΔC_{soil} was set constant as the average annual belowground carbon increase since afforestation (Qubaja et al., in press).

2.6. Statistical analyses

Tow-way ANOVA tests were performed at a significance level set at $p = 0.001$ to detect significant effects of locations (OA, BT, and UT), sites, and their interactions on Rs and metrological parameters. Pearson correlation analysis (r) was used to detect the correlation between Rs and meteorological parameters. To quantify spatio-temporal variability in Rs, the coefficient of variation (CV%) was calculated as [(STDEV/Mean)*100%]. Heterogeneity was considered weak if CV% ≤ 10%, moderate if 10% < CV% ≤ 100%, and strong if CV% > 100%. All the analyses were performed using Matlab software, Version R2017b (MathWorks, Inc., MA, USA).

3. Results

3.1. Spatial variations

The spatial variations in Rs across locations (distance from nearest tree) and sites (across the study area) are reported in Table 1, together with other measured variables. The results indicated an overall mean Rs value of 0.8 ± 0.1 μmol m^{-2} s^{-1}, with distinct values for the three locations. Rs was greater at UT locations than at the BT and OA locations by a factor of ~2. The spatial variability among the locations was also apparent in the Rs daily cycle (Fig. 1), with clear differences between the wet season (November to April), when the UT showed consistently higher Rs values than at other locations by a factor of about 1.6 and the dry season by a factor of approximately 2.6. Note that the daily peak in Rs remained at midday in both the wet and dry seasons. Overall, the 21 collars showed moderate variations (CV = 55%; Table 1), Rs was negatively correlated with distance from trees (Dt; $r = 0.62$; $p < 0.01$) and with soil and air temperatures (Ts and Ta; $r = 0.45$; $p < 0.05$), and positively correlated with soil water content and relative humidity (SWC and RH; $r = 0.50$; $p < 0.05$). The inverse correlation between Rs and distance from the nearest tree could be useful in considering the expected decline in stand density due to thinning and mortality (e.g., associated with a drying climate). For a first approximation, the results indicate that decreasing from the present stand density of 300 trees ha^{-1} to 100 trees ha^{-1} and the resulting increase in mean distance among trees could result in decreasing ecosystem Rs by 11%.

313 **Table 1** Annual mean of half-hour values across locations (OA, open area; BT, between trees; UT, under tree) in
314 seven sites in the forest during the study period, of soil respiration flux rates (Rs) together with the soil water content
315 at 10 cm depth (SWC), minimum distances from nearby tree (Dt), soil temperature at 5 cm depth (Ts), and air
316 temperature (Ta) and relative humidity (RH) at the soil surface (numbers in parenthesis indicate ±se).

Locations	Sites	Rs [μmol m^{-2} s^{-1}]	SWC [x100 m^3 m^{-3}]	Dt [m]	Ts [ºC]	Ta [ºC]	RH [%]
OA	1	1.64 (0.02)	16.5 (0.2)	2.9	15.6 (0.1)	15.4 (0.2)	59.7 (0.5)
	2	0.72 (0.01)	14.5 (0.2)	3.6	15.9 (0.2)	15.0 (0.2)	58.4 (0.6)
	3	1.23 (0.02)	19.3 (0.2)	7.0	20.6 (0.3)	18.2 (0.2)	53.5 (0.5)
	4	0.38 (0.01)	11.3 (0.2)	3.0	22.6 (0.2)	20.8 (0.1)	58.9 (0.4)
	5	0.38 (0.01)	5.8 (0.2)	3.0	25.5 (0.1)	24.0 (0.1)	43.1 (0.4)
	6	0.31 (0.01)	5.7 (0.4)	2.8	30.0 (0.3)	26.2 (0.3)	51.8 (0.9)
	7	0.14 (0.01)	6.1 (0.3)	3.5	25.5 (0.2)	23.2 (0.3)	44.5 (0.9)
	Average	**0.68 (0.21)**	**11 (0)**	**3.7 (0.6)**	**22.3 (2.0)**	**20.4 (1.6)**	**52.8 (2.6)**
	CV [%]	**81 %**	**50%**	**41%**			**13 %**
BT	1	0.77 (0.01)	10.5 (0.2)	1.8	16.1 (0.1)	15.2 (0.2)	60.5 (0.5)
	2	0.88 (0.01)	12.1 (0.2)	1.5	14.8 (0.2)	14.7 (0.2)	59.5 (0.6)
	3	0.84 (0.01)	20.4 (0.2)	2.7	20.1 (0.3)	18.4 (0.2)	54.1 (0.6)
	4	0.91 (0.01)	14.4 (0.2)	2.7	23.3 (0.2)	21.3 (0.2)	58.5 (0.4)
	5	0.41 (0.00)	3.9 (0.2)	2.0	24.6 (0.1)	24.0 (0.1)	43.2 (0.4)
	6	0.41 (0.01)	3.3 (0.4)	2.5	29.1 (0.2)	26.0 (0.3)	52.5 (0.8)
	7	0.46 (0.01)	5.5 (0.3)	1.2	23.9 (0.1)	22.8 (0.3)	45.7 (0.9)
	Average	**0.67 (0.09)**	**10 (0)**	**2.0 (0.2)**	**21.7 (1.9)**	**20.3 (1.6)**	**53.4 (2.6)**
	CV [%]	**35 %**	**63%**	**29%**			**13 %**
UT	1	1.22 (0.02)	9.3 (0.2)	0.2	15.7 (0.1)	15.2 (0.2)	60.0 (0.5)
	2	1.42 (0.01)	14.0 (0.2)	0.3	14.8 (0.2)	14.8 (0.2)	59.4 (0.6)
	3	1.64 (0.01)	19.8 (0.2)	0.5	19.0 (0.2)	18.0 (0.2)	54.5 (0.6)
	4	1.90 (0.02)	11.3 (0.2)	0.6	22.0 (0.1)	20.8 (0.1)	59.0 (0.4)
	5	1.16 (0.01)	4.0 (0.2)	0.4	23.9 (0.1)	23.7 (0.1)	44.1 (0.4)
	6	1.29 (0.01)	4.5 (0.4)	0.2	29.5 (0.3)	25.9 (0.3)	52.7 (0.9)
	7	0.89 (0.01)	5.2 (0.3)	0.2	25.0 (0.1)	23.0 (0.3)	45.5 (0.9)
	Average	**1.36 (0.13)**	**10 (0)**	**0.3 (0.1)**	**21.4 (2.0)**	**20.2 (1.6)**	**53.6 (2.5)**
	CV [%]	**25 %**	**60%**	**46%**			**12 %**
All	**Average (SE)**	**0.8 (0.1)**	**11 (0)**	**2.0 (0.4)**	**21.8 (1.1)**	**20.3 (0.9)**	**53.3 (1.4)**
	Max	**1.90**	**20**	**7.0**	**30.0**	**26.2**	**60.5**
	Min	**0.14**	**3**	**0.2**	**14.8**	**14.7**	**43.1**
	CV [%]	**55 %**	**55%**	**82%**			**12 %**
Two-way ANOVA (*P* value)	**Site**	**0.000**	**0.000**		**0.000**	**0.000**	**0.000**
	Location	**0.000**	**0.000**		**0.000**	**0.220**	**0.074**
	Site x Location	**0.000**	**0.000**		**0.000**	**0.645**	**0.961**
Pearson Correlation with Rs			**.50***	**-.62****	**-.45***	**-.45***	**.50***

317 **. Correlation is significant at the 0.01 level (two-tailed).
318 *. Correlation is significant at the 0.05 level (two-tailed).

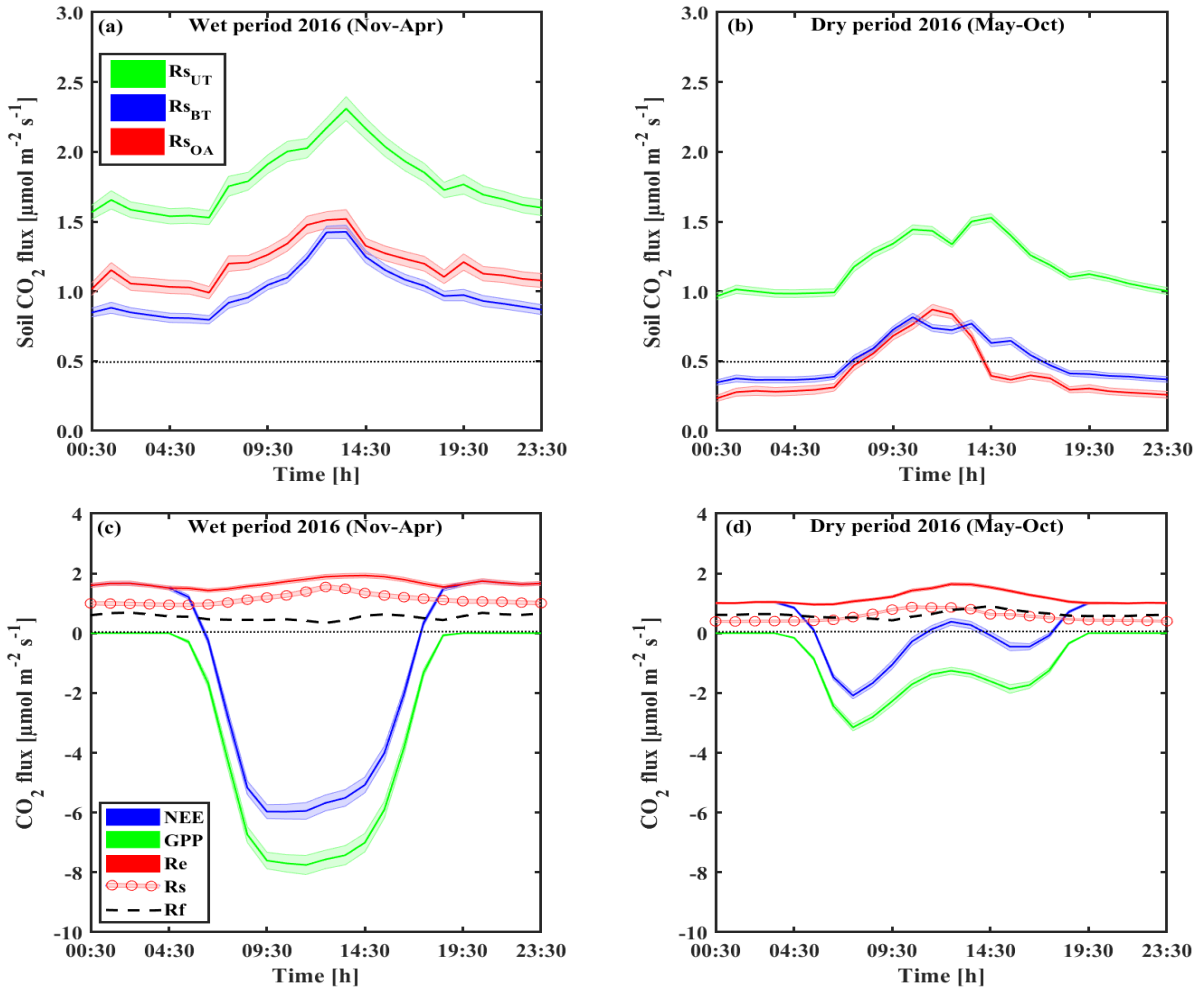

Figure 1 Representative diurnal cycles of soil respiration (Rs; using soil chambers across locations: open area, OA; between trees, BT; under trees, UT) and sites in panels a and b, of net ecosystem exchange (NEE; canopy scale eddy covariance) and gross primary production (GPP), and ecosystem respiration (Re) and its partitioning to soil respiration (Rs) and aboveground tree respiration (Rf) in panels c and d, during the wet (Nov–Apr) and dry (May–Oct) periods. Based on half-hour values over the diurnal cycle; shaded areas indicate ±se; Rf was estimated as the residual as Rf = Re-Rs and was presented as a dashed line.

3.2. Temporal dynamics

On the diurnal timescale, CO_2 fluxes showed typical daily cycles (Fig. 1). As expected, on average, all CO_2 fluxes were higher during the wet period compared to the dry season by a factor of ~2. However, Rs and Re peaked around midday in both the wet and dry seasons, while the more physiologically controlled NEE and GPP showed a shift from midday (around 11:00–14:00) to early morning (08:00–11:00) in the dry season, with a midday depression and a secondary afternoon peak (Fig. 1d).

The temporal variations across the seasonal cycle are reported in Fig. 2, based on monthly mean values, exhibiting sharp differences between the wet and dry seasons. As previously observed in this semi-arid site, all CO_2 fluxes peak in early spring between March and April. The corresponding high-resolution data

are reported in Fig. SI-6, which show also that the high winter (February) Rs rates were associated with clear days when photosynthetic active radiation (PAR) increased with air temperature, Ta. These data also show that, following rainy days, daily Rs values could reach 6.1 µmol m^{-2} s^{-1}, although the average was 1.1 ± 0.2 µmol m^{-2} s^{-1} during the wet period, which diminished by ~55% in the dry season to mean daily values of 0.5 ± 0.1 µmol m^{-2} s^{-1}. In spring (April), all CO_2 fluxes peaked during the crossover trends of decreasing soil moisture content and increasing both temperature and PAR (Fig. SI-6).

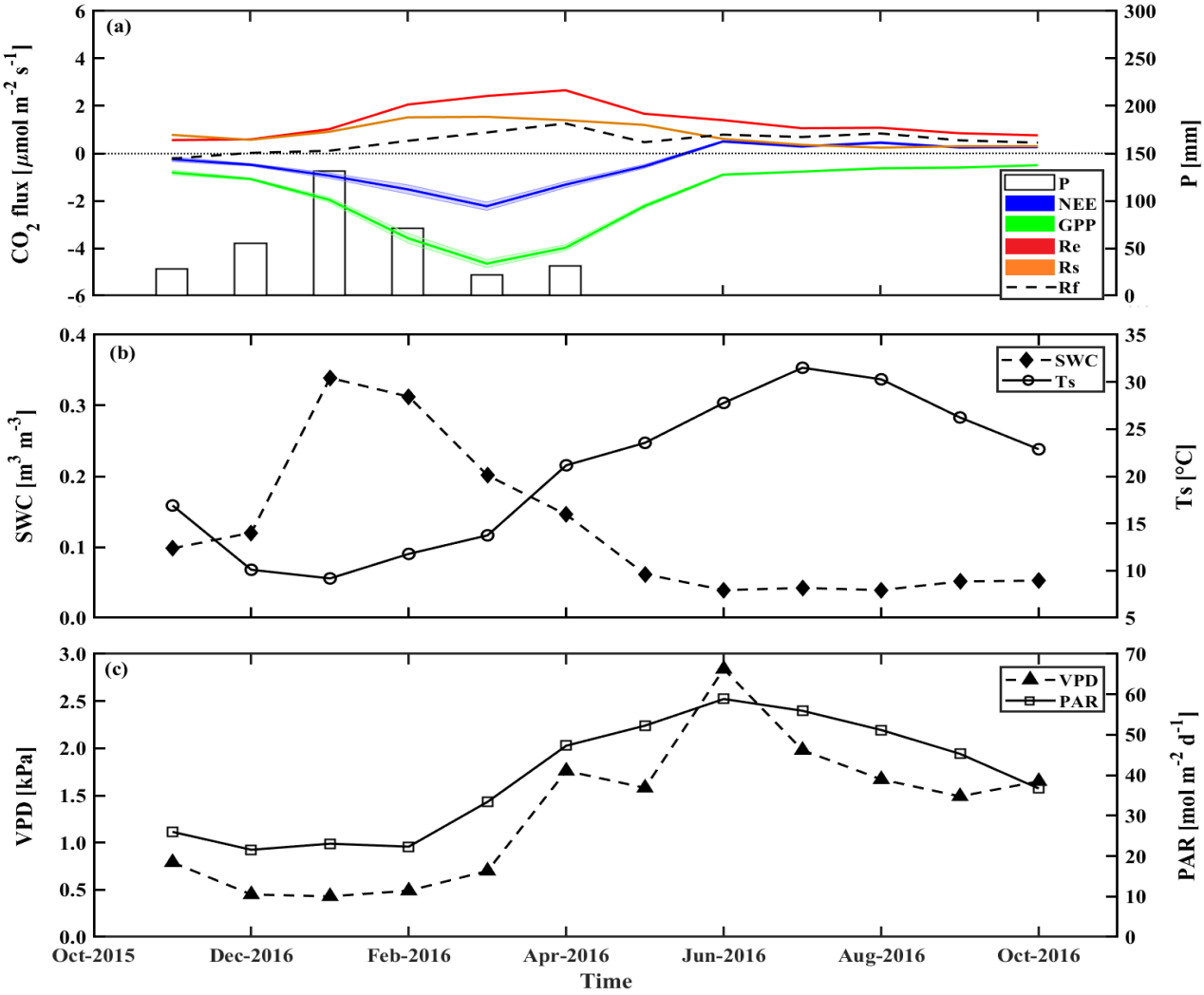

Figure 2 Seasonal trends of monthly mean values during the research period of a) the fluxes of net ecosystem exchange (NEE), gross primary production (GPP), and ecosystem respiration (Re) and its components, soil respiration (Rs) and aboveground tree respiration (Rf); and monthly mean of key environmental parameters, b) soil water content at the top 10 cm ($SWC_{0\text{-}10}$) and soil temperature at 5 cm (Ts), and c) vapor pressure deficit (VPD) and photosynthetic activity radiation (PAR). Rf is obtained from the Re-Rs.

The temporal variations in the half-hour values of Rs reflected changes in soil moisture at 0–5 cm depth and PAR (r = 0.5 and 0.2, respectively; $p < 0.01$) and negative correlations with Ts and RH (r = 0.2 and 0.1, respectively; $p < 0.01$). The variations in the integrated Rs showed a CV of 71%, with the temporal

variations dominated strongly by PAR (CV > 100%), moderately by SWC (CV~85%), and weakly by RH (CV~40%). Repeating the models applied by Grünzweig et al. (2009), the potential climatic factors that best predicted daily Rs shifted from SWC and PAR in the dry season to Ts and PAR in the wet season (Table SI-2). These equations explained 43% and 70% of the variation in Rs in the dry and wet seasons, respectively (Table SI-2). A reasonable forecast of the temporal variations in Rs (μmol m^{-2} s^{-1}) at half-hour values (R^2 = 0.60, p < 0.0001) was obtained based on $SWC_{0\text{-}10}$ and Ts values across the entire seasonal cycle, based on:

$$Rs = 0.05126 * \exp(0.04274 * Ts + 28.51 * SWC - 74.44 * SWC^2) \quad (13)$$

At the ecosystem scale, Re was characterized by high fluxes in the wet season and peak values of ~2.4 μmol m^{-2} s^{-1} in February to April (Fig. 2; Table SI-1). Refluxes rapidly decreased after the cessation of rain and reached the lowest values in the fall (September to October), with mean dry period values of 0.5 ± 0.1 μmol m^{-2} s^{-1} (Fig. 2, Table SI-1). GPP had a mean value of -1.8 ± 0.4 μmol m^{-2} s^{-1}, and daily NEE had a mean value of -0.5 ± 0.3 μmol m^{-2} s^{-1} (Table SI-1 and Fig. SI-6), with the same seasonality (Fig. 2).

Table 2 $\delta^{13}C$ and $\Delta^{14}C$ signature of soil respiration (Rs) and its partitioning to autotrophic (Rsa), heterotrophic (Rh), and abiotic (Ri), together with the relative contribution of each to the soil and ecosystem respiration for Yatir forest during eight campaigns of measurements from January to September 2016 (numbers in parenthesis indicate ±se) in comparison to results obtained previously in the same forest (2001–2006 mean values). The monthly contribution of Rsa, Rh, and Ri to Rs or Re is presented in Fig. 3a and b, respectively.

Signature	**Rsa**	**Rh**	**Ri**	**Rs**
			[‰]	
$\delta^{13}C$	-23.7 (0.5)[1]	-24.3 (0.0)[1]	-6.5 (0.0)[1]	-20.8 (±0.6)[1]
$\Delta^{14}C$	30[3]	50[3]	-900[2]	-134 (34)[4]
Relative contribution to Rs (2015–2016)	**0.40 (0.02)**	**0.39 (0.02)**	**0.21 (0.04)**	
Relative contribution to Re (2015–2016)	**0.24 (0.04)**	**0.23 (0.04)**	**0.13 (0.01)**	**0.60 (0.06)**

[1] Measured in the present study; [2] measured by Carmi et al., (2013); [3] calculated based on the measured atmospheric value by Carmi et al. (2013); and [4] calculated based on the best fit regression equation in Fig. SI-2.

Figure 3 (see also Table 2) summarizes the seasonal variations in Rs and Re partitioning. The monthly Rsa and Rh were not significantly different but were significantly different from Ri (p < 0.05). The Rsa/Rs ratios ranged from 0.32 to 0.46, the largest contribution occurring in early spring from February to April. The Rh/Rs fraction ranged between 0.33 and 0.45, being highest during the wet season. The Ri/Rs – the fraction of inorganic sources from the total soil respiration – ranged from 0.09 to 0.35, the largest contribution being in the driest period. The mean relative contributions of these components to Rs over the sampling campaigns are presented in Figure 3a, but, on average, soil biotic fluxes were higher than abiotic fluxes by a factor of ~4. Repartitioning showed an average increase in Rf/Re from 25% in the wet season to 54% in the dry season and a decline in Rs/Re from 75% to 46% on average in the wet and the dry seasons, respectively, which reflected a seasonal change of Rf in the wet season to peak values in the dry season (Fig. 3b). Both the highest and lowest Rs fractions (~0.74 and nearly 0.34) along the seasonal cycle

were associated with low total Re fluxes, that is, in the fall before the Rf peak in the spring and in the summer, when physiological controls limited water loss.

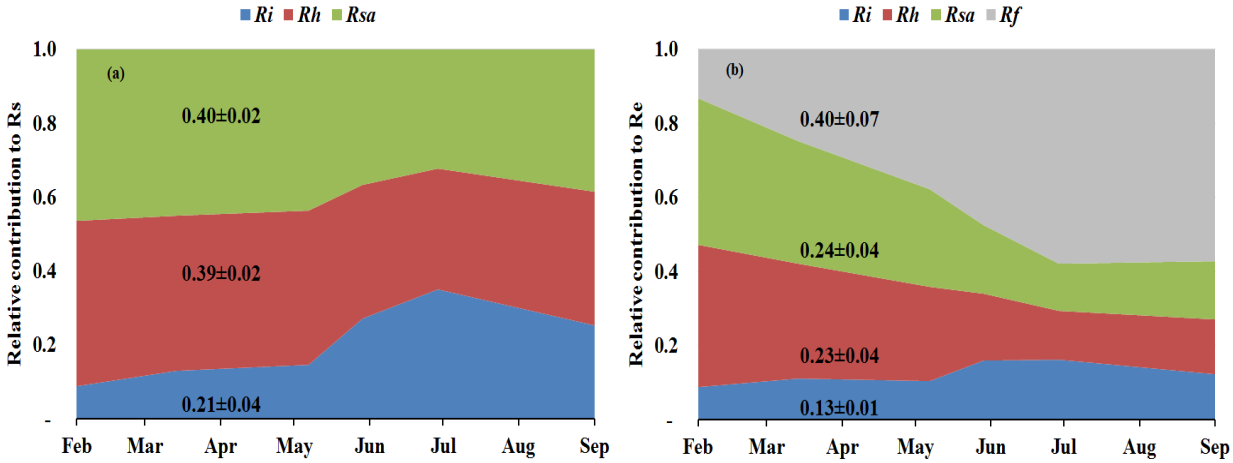

Figure 3 a) Linear mixing models $\delta^{13}C$ and $\Delta^{14}C$ of soil respiration (Rs) isotope signatures (from soil CO_2 profile method at 0, 30, 60, 90, and 120 cm soil depth) were used to determine the seasonal variations in the relative contribution of soil autotrophic (Rsa), heterotrophic (Rh), and abiotic (Ri) components to Rs, and b) seasonal variations in the relative contribution of soil autotrophic (Rsa), heterotrophic (Rh), abiotic (Ri), and foliage and stem respiration (Rf is obtained from the Re-Rs) components to ecosystem respiration (Re) during eight campaigns (Jan–Sep) in 2016. These results confirmed earlier estimates of Grünzweig et al. (2009) and Maseyk et al. (2008a).

3.3. Annual scale

Table 3 Mean annual values of ecosystem respiration (Re), its components and associated ratios, net ecosystem exchange (NEE; from eddy covariance), net primary productivity (NPP), gross primary productivity (GPP), carbon-use efficiency (CUE), leaf area index (LAI), and ratio of total belowground carbon allocation (TBCA) to GPP (TBCA/GPP) in the present study (mean of Nov 2015 to Oct 2016) and in comparison to results obtained previously in the same forest (2001–2006 mean values). Ri, Rh, Rsa, Rs, Rl and Rw denote abiotic, heterotrophic, soil autotrophic, soil, foliage, and wood CO_2 flux, respectively. Q_{10} is derived during the two studies for the wet and dry season.

Study	Rs	Rh	Rsa	Rl	Rw	Ri	Re	NEE	NPP	GPP
					[g m^{-2} y^{-1}]					
Mean (2001–2006)	406	147	203	260	70	56	735	-211	-358	-880
x/Rs		0.36	0.50			0.14				
x/Re	0.55	0.20	0.28	0.35	0.10	0.07				
Mean (2015–2016)	295	115	119	155	39	61	488	-167	-282	-655
x/Rs		0.39	0.40			0.21				
x/Re	0.60	0.23	0.24	0.32	0.08	0.13				
Ratio of $(x/Rs)_{2016}/(x/Rs)_{2003}$		**1.08**	**0.81**			**1.50**				
Ratio of $(x/Re)_{2016}/(x/Re)_{2003}$	**1.09**	**1.18**	**0.88**	**0.90**	**0.84**	**1.64**				

Study	Q_{10}		CUE	TBCA/GPP[3]	LAI
	SWC[1]	SWC[2]			[m^2 m^{-2}]
Mean (2001–2006)	2.5	1.2	0.40	0.41	1.3
Mean (2015–2016)	1.6	1.1	0.43	0.38	2.1
Ratio of x_{2016}/x_{2003}	**0.64**	**0.92**	**1.06**	**0.93**	**1.62**

[1] SWC ≥ 0.2 [m^3 m^{-3}] and [2] SWC < 0.2 [m^3 m^{-3}]; [3] and the mean of GPP used by Grünzweig et al., 2009 to estimate the TBCA/GPP was 834 g m^{-2} y^{-1}.

On an annual timescale, estimates of CO_2 flux components based on EC measurements resulted in annual values of GPP, NPP, Re, and NEP of 655, 282, 488, and 167 g C m^{-2} y^{-1}, respectively (Tables 3 and SI-1). On average across the measurement period, Rs was the main CO_2 flux to atmosphere, making up 60 ± 6% of Re (295 ± 4 g C m^{-2} y^{-1}; Tables 3 and SI-1), and Rf was another significant component accounting for 40 ± 6% of Re (Fig. 3b), which reflected the low density (300 trees ha^{-1}) nature of the semi-arid forest. As indicated above, Re partitioning showed a decrease in Rs/Re and an increase in Rf/Re from winter to summer, which is clearly apparent in Fig. 3b. On an annual scale, during the study period, estimates of Rf, Rsa, Rh, and Ri values were 194 ± 36, 119 ± 21, 115 ± 20, and 61 ± 6 g C m^{-2} y^{-1}, respectively. Despite relatively high rates of respiration fluxes, the CUE of the ecosystem remained high at 0.43.

Using the site records of nearly 20 years, long-term trends in GPP, NPP, Re, and NEP were obtained. Soil respiration and its partitioning could not be similarly monitored continuously, but combining the present results with the 2001–2006 values obtained by Grünzweig et al. (2009) and Maseyk et al. (2008a) provided a basis for estimating the long-term trends in soil respiration. Notably, no clear or significant trend over time was observed in any of the canopy-scale continuously monitored fluxes, but, because of relatively large interannual variations, associated mainly with those in precipitation (see Qubaja et al., in press), it is likely that the relative contributions of the different fluxes, expressed as ratios in Table 3, provide a more robust perspective of the long-term temporal changes in the ecosystem functioning. The results presented n Table 3 reflect the long-term growth of the forest, with a relatively large increase in LAI, but the belowground allocation remained around 40%. The ratio of the respiration components to total ecosystem respiration, Re, or to GPP indicated little change in the total soil respiration, Rs, component, but a general shift from the autotrophic components Rsa, Rl, and Rw to the heterotrophic component, Rh, across the 13-year observation period noted above (with the mean values for 2011–2005 assigned to 2003 and the new data to 2016).

4. Discussion

Partitioning ecosystem carbon fluxes and long-term observational studies are key to understanding ecosystem carbon dynamics and their response to change. Overall, the results support our research hypothesis that the observed high CUE at our site is at least partly due to the characteristics of the carbon flux partitioning that can be associated with the semi-arid conditions. Compared to other sites and climates (see comparative compilation in Table SI-3), the results reflect several key points: 1) relatively high belowground allocation; 2) low soil respiration in general, and low heterotrophic respiration in particular; 3) combining the results for 2016 and those of our earlier study offered a long-term perspective across 13 years, indicating that the low Rs in this ecosystem is robust and exhibits reduced sensitivity to temperature, and 4) there is a general long-term shift from autotrophic to heterotrophic respiration.

Comparing CO_2 fluxes in this forest with fluxes in a range of European forests showed that mean NEP in the semi-arid forest (167 g C m^{-2} y^{-1}) is similar to the mean NEP in other European forests (150 g C m^{-2} y^{-1}; FLUXNET).

Carbon partitioning belowground (TBCA/GPP) was relatively high (~38%), with little change across the long-term observation period. It is, however, within the range of mean value for forests in different biomes (Litton et al., 2007). High belowground allocation helps explain the high rate of SOC accumulation observed over the period since afforestation (Grünzweig et al., 2007; Qubaja et al., in press). Note that, irrespective of the soil carbon accumulation, the abiotic component to the CO_2 flux seems to be significant in dry environments (Table 3) and in particular in the dry seasons, when biological activities drastically decrease (Kowalski et al., 2008; Lopez-Ballesteros et al., 2017; Serrano-Ortiz et al., 2010; Martí-Roura et al., 2019). The results show that considering the abiotic effects on estimating soil respiration and, in turn, on estimating the carbon budget in dry calcareous soils can play an important part in estimating soil and ecosystem respiration fluxes (Angert et al., 2015; Roland et al., 2012).

The soil CO_2 efflux in the semi-arid forest (295 g C m^{-2} y^{-1}) is at the low end of Rs values across the range of climatic regions, from 50 to 2,750 g C m^{-2} y^{-1} (Adachi et al., 2017; Chen et al., 2014; Grünzweig et al., 2009; Hashimoto et al., 2015). This is clearly lower than the mean Rs value for global evergreen needle forests, which is estimated at 690 g C m^{-2} y^{-1} (Chen et al., 2014), and between estimates for desert scrub and Mediterranean woodland (224–713 g C m^{-2} y^{-1}; Raich and Schlesinger, 1992) or for Mediterranean forests (561–1,015 g C m^{-2} y^{-1}; Casals et al., 2011; Luyssaert et al., 2007; Matteucci et al., 2015; Misson et al., 2010; Rey et al., 2002; Rodeghiero and Cescatti, 2005). The mean instantaneous rate of Rs, 0.8 µmol m^{-2} s^{-1}, is also in the range reported for unmanaged forest and grassland in the dry Mediterranean region (0.5 and 2.1 µmol m^{-2} s^{-1}; Correia et al., 2012).

The observed low Rs values were associated with a relatively high fraction of autotrophic and a lower fraction of heterotrophic respiration. The mean annual-scale Rsa/Rs ratio of 0.40 was at the high end of the global range of 0.09 to 0.49 (Chen et al., 2014; Hashimoto et al., 2015). In contrast, heterotrophic respiration showed an annual-scale Rh/Rs ratio of 0.39 ± 0.02 (Table 2 and Fig. 3), which is lower than the estimated global mean Rh/Rs value of 0.56 (Hashimoto et al., 2015), but within the range of Mediterranean region forest, which varies between 0.29 to 0.77 (Casals et al., 2011; Luyssaert et al., 2007; Matteucci et al., 2015; Misson et al., 2010; Rey et al., 2002; Rodeghiero and Cescatti, 2005). The relatively low annual scale of the heterotrophic respiration to Rs is consistent with the dry soil over much of the year in this forest (Figs 2 and SI-6) and the observed low decomposability of plant detritus and high mean SOC accumulation rate (Grünzweig et al., 2007).

The long-term perspective from the 13-year observation period indicates emerging trends that can be a basis for assessing the effects of forest age and the marked increase in LAI (Table 3) and changes in environmental conditions (generally warming and drying; see, e.g., Lelieveld et al., 2012). As noted above, comparing the non-continuous data from the present (2016) and earlier (2001–2006) studies is sensitive to the large interannual variations in the ecosystem activities and fluxes (Qubaja et al., in press), and we therefore focused on the more robust changes in the ratio of the respiration components to the overall fluxes (Re) (Table 3). This shows a shifting trend from the autotrophic components to the heterotrophic, with little change in the contribution of Rs to the overall efflux. The ratios of Rsa, Rl, and Rw to Re tended to decrease by about 13%, while that of Rh increased by about 18%; similar trends were seen in soil respiration, with Rsa/Rs decreasing by -19% and Rh/Rs increasing by +8% (Table 3). The relatively low Rs under conditions of high temperature in the semi-arid ecosystem implies reduced sensitivity of respiration to temperature. This is partly imposed by low SWC conditions during extended parts of the year (Grünzweig et al., 2009; cf. Rey et al., 2002; Xu and Qi, 2001). Accordingly, Rs showed greater sensitivity to Ts in the wet period, but during the 8–9 months of the year when SWC was below ~0.2 m^3 m^{-3}, Rs varied predominantly with water availability. The long-term perspective reported in Table 3 indicates a further decrease in temperature sensitivity, with mean Q_{10} values in the dry season decreasing from 1.6 to 1.1. These estimated Q_{10} values are generally consistent with published values for different ecosystems (1.4 to 2.0; Hashimoto et al., 2015; Zhou et al., 2009) and with low values under low SWC (Reichstein et al., 2003; Tang et al., 2005). This is also consistent with soil warming experiments by 0.76°C in Mediterranean ecosystems, which decreased the Rs by 16%, and Q_{10} by 14% (Wang et al., 2014). Note also that the low temperature sensitivity in the dry season is likely to be related to reduced microbial activity, but may also involve downregulation of plant activity (Maseyk et al., 2008a) and drought-induced dormancy of shallow roots (Schiller, 2000). Finally, we also note that the greater importance of moisture availability in influencing respiration is clearly apparent from the observed relationships of Rs and Rh to mean annual precipitation (MAP) in European evergreen needle forests (Fig. SI-8; see also Grünzweig et al., 2007), which are not observed with respect to mean annual temperature.

Data availability

The data used in this study are archived and available from the corresponding author upon request (dan.yakir@weizmann.ac.il).

Author contributions

RQ and DY designed the study; RQ, FT, ER and DY performed the experiments. RQ and DY analyzed the data. DY and RQ wrote the paper, with discussions and contributions to interpretations of the results from all co-authors.

Competing interests

The authors declare that they have no conflict of interest.

5. Acknowledgements

This long-term study was funded by the Forestry Department of Keren-Kayemeth-LeIsrael (KKL) and the German Research Foundation (DFG)m as part of the project "Climate feedback and benefits of semi-arid forests" (CliFF) and by the Israel Ministry of Science and the Ministry of National Education, Higher Education, and Research (MENESR) of France (IMOS-French Program: 3-6735). The authors thank Efrat Schwartz for assistance with lab work. The long-term operation of the Yatir Forest Research Field Site is supported by the Cathy Wills and Robert Lewis Program in Environmental Science. We thank the entire Yatir team for technical support and the local KKL personnel for their cooperation.

6. References

Adachi, M., Ito, A., Yonemura, S., & Takeuchi, W. (2017). Estimation of global soil respiration by accounting for land-use changes derived from remote sensing data. Journal of Environmental Management, 200, 97-104.

Angert, A., Yakir, D., Rodeghiero, M., Preisler, Y., Davidson, E. A., & Weiner, T. (2015). Using O-2 to study the relationships between soil CO2 efflux and soil respiration. Biogeosciences, 12(7), 2089-2099.

Aubinet, M., Grelle, A., Ibrom, A., Rannik, U., Moncrieff, J., Foken, T., et al. (2000). Estimates of the annual net carbon and water exchange of forests: The EUROFLUX methodology. Advances in Ecological Research, Vol 30, 30, 113-175.

Bahn, M., Janssens, I. A., Reichstein, M., Smith, P., & Trumbore, S. E. (2010). Soil respiration across scales: towards an integration of patterns and processes. New Phytologist, 186(2), 292-296.

Balogh, J., Pinter, K., Foti, S., Cserhalmi, D., Papp, M., & Nagy, Z. (2011). Dependence of soil respiration on soil moisture, clay content, soil organic matter, and CO2 uptake in dry grasslands. Soil Biology & Biochemistry, 43(5), 1006-1013.

Binkley, D., Stape, J. L., Takahashi, E. N., & Ryan, M. G. (2006). Tree-girdling to separate root and heterotrophic respiration in two Eucalyptus stands in Brazil. Oecologia, 148(3), 447-454.

Bonan, G. B. (2008). Ecological climatology : concepts and applications (2nd ed.. ed.). Cambridge: Cambridge : Cambridge University Press.

Bond-Lamberty, B., & Thomson, A. (2010). Temperature-associated increases in the global soil respiration record. Nature, 464(7288), 579-U132.

Buchmann, N. (2000). Biotic and abiotic factors controlling soil respiration rates in Picea abies stands. Soil Biology & Biochemistry, 32(11-12), 1625-1635.

Carbone, M. S., Winston, G. C., & Trumbore, S. E. (2008). Soil respiration in perennial grass and shrub ecosystems: Linking environmental controls with plant and microbial sources on seasonal and diel timescales. Journal of Geophysical Research-Biogeosciences, 113(G2).

Carmi, I., Yakir, D., Yechieli, Y., Kronfeld, J., & Stiller, M. (2013). VARIATIONS IN SOIL CO2 CONCENTRATIONS AND ISOTOPIC VALUES IN A SEMI-ARID REGION DUE TO BIOTIC AND ABIOTIC PROCESSES IN THE UNSATURATED ZONE. Radiocarbon, 55(2-3), 932-942.

Carvalhais, N., Forkel, M., Khomik, M., Bellarby, J., Jung, M., Migliavacca, M., et al. (2014). Global covariation of carbon turnover times with climate in terrestrial ecosystems. Nature, 514(7521), 213-+.

Casals, P., Lopez-Sangil, L., Carrara, A., Gimeno, C., & Nogues, S. (2011). Autotrophic and heterotrophic contributions to short-term soil CO2 efflux following simulated summer precipitation pulses in a Mediterranean dehesa. Global Biogeochemical Cycles, 25. doi:10.1029/2010gb003973

Chen, D., Zhang, Y., Lin, Y., Zhu, W., & Fu, S. (2010). Changes in belowground carbon in Acacia crassicarpa and Eucalyptus urophylla plantations after tree girdling. Plant and Soil, 326(1-2), 123-135.

Chen, S. T., Zou, J. W., Hu, Z. H., Chen, H. S., & Lu, Y. Y. (2014). Global annual soil respiration in relation to climate, soil properties and vegetation characteristics: Summary of available data. Agricultural and Forest Meteorology, 198, 335-346.

Conant, R. T., Klopatek, J. M., Malin, R. C., & Klopatek, C. C. (1998). Carbon pools and fluxes along an environmental gradient in northern Arizona. Biogeochemistry, 43(1), 43-61.

Correia, A. C., Minunno, F., Caldeira, M. C., Banza, J., Mateus, J., Carneiro, M., . . . Pereira, J. S. (2012). Soil water availability strongly modulates soil CO2 efflux in different Mediterranean ecosystems: Model calibration using the Bayesian approach. Agriculture Ecosystems & Environment, 161, 88-100. doi:10.1016/j.agee.2012.07.025

Davidson, E. A., & Janssens, I. A. (2006). Temperature sensitivity of soil carbon decomposition and feedbacks to climate change. Nature, 440(7081), 165-173.

DeLucia, E. H., Drake, J. E., Thomas, R. B., & Gonzalez-Meler, M. (2007). Forest carbon use efficiency: is respiration a constant fraction of gross primary production? Global Change Biology, 13(6), 1157-1167.

Deng, Q., Hui, D., Zhang, D., Zhou, G., Liu, J., Liu, S., et al. (2012). Effects of Precipitation Increase on Soil Respiration: A Three-Year Field Experiment in Subtropical Forests in China. Plos One, 7(7).

Etzold, S., Ruehr, N. K., Zweifel, R., Dobbertin, M., Zingg, A., Pluess, P., et al. (2011). The Carbon Balance of Two Contrasting Mountain Forest Ecosystems in Switzerland: Similar Annual Trends, but Seasonal Differences. Ecosystems, 14(8), 1289-1309.

Etzold, S., Zweifel, R., Ruehr, N. K., Eugster, W., & Buchmann, N. (2013). Long-term stem CO2 concentration measurements in Norway spruce in relation to biotic and abiotic factors. New Phytologist, 197(4), 1173-1184. doi:10.1111/nph.12115

Falge, E., Baldocchi, D., Tenhunen, J., Aubinet, M., Bakwin, P., Berbigier, P., et al. (2002). Seasonality of ecosystem respiration and gross primary production as derived from FLUXNET measurements. Agricultural and Forest Meteorology, 113(1-4), 53-74.

Flechard, C. R., Ibrom, A., Skiba, U. M., de Vries, W., van Oijen, M., Cameron, D. R., et al. (2019). Carbon / nitrogen interactions in European forests and semi-natural vegetation. Part I: Fluxes and budgets of carbon, nitrogen and greenhouse gases from ecosystem monitoring and modelling, Biogeosciences Discuss., https://doi.org/10.5194/bg-2019-333, in review, 2019.

Flechard, C. R., van Oijen, M., Cameron, D. R., de Vries, W., Ibrom, A., Buchmann, N., Dise, N. B., et al. (2019). Carbon / nitrogen interactions in European forests and semi-natural vegetation. Part II: Untangling climatic, edaphic, management and nitrogen deposition effects on carbon sequestration potentials, Biogeosciences Discuss., https://doi.org/10.5194/bg-2019-335, in review, 2019.

Frank, A. B., Liebig, M. A., & Hanson, J. D. (2002). Soil carbon dioxide fluxes in northern semiarid grasslands. Soil Biology & Biochemistry, 34(9), 1235-1241.

Frey, B., Hagedorn, F., & Giudici, F. (2006). Effect of girdling on soil respiration and root composition in a sweet chestnut forest. Forest Ecology and Management, 225(1-3), 271-277.

Gelfand, I., Grünzweig, J. M., & Yakir, D. (2012). Slowing of nitrogen cycling and increasing nitrogen use efficiency following afforestation of semi-arid shrubland. Oecologia, 168(2), 563-575. doi:10.1007/s00442-011-2111-0

Giardina, C. P., & Ryan, M. G. (2002). Total belowground carbon allocation in a fast-growing Eucalyptus plantation estimated using a carbon balance approach. Ecosystems, 5(5), 487-499.

Graven, H. D., Guilderson, T. P., & Keeling, R. F. (2012). Observations of radiocarbon in CO2 at La Jolla, California, USA 1992-2007: Analysis of the long-term trend. Journal of Geophysical Research-Atmospheres, 117.

Grünzweig, J. M., Gelfand, I., Fried, Y., & Yakir, D. (2007). Biogeochemical factors contributing to enhanced carbon storage following afforestation of a semi-arid shrubland. Biogeosciences, 4(5), 891-904.

Grünzweig, J. M., Hemming, D., Maseyk, K., Lin, T., Rotenberg, E., Raz-Yaseef, N., et al. (2009). Water limitation to soil CO2 efflux in a pine forest at the semiarid "timberline". Journal of Geophysical Research-Biogeosciences, 114.

Grünzweig, J. M., Lin, T., Rotenberg, E., Schwartz, A., & Yakir, D. (2003). Carbon sequestration in arid-land forest. Global Change Biology, 9(5), 791-799.

Hagedorn, F., Joseph, J., Peter, M., Luster, J., Pritsch, K., Geppert, U., . . . Arend, M. (2016). Recovery of trees from drought depends on belowground sink control. Nature Plants, 2(8). doi:10.1038/nplants.2016.111

Hashimoto, S., Carvalhais, N., Ito, A., Migliavacca, M., Nishina, K., & Reichstein, M. (2015). Global spatiotemporal distribution of soil respiration modeled using a global database. Biogeosciences, 12(13), 4121-4132.

Hemming, D., Yakir, D., Ambus, P., Aurela, M., Besson, C., Black, K., . . . Vesala, T. (2005). Pan-European delta C-13 values of air and organic matter from forest ecosystems. Global Change Biology, 11(7), 1065-1093. doi:10.1111/j.1365-2486.2005.00971.x

Hogberg, P., Bhupinderpal, S., Lofvenius, M. O., & Nordgren, A. (2009). Partitioning of soil respiration into its autotrophic and heterotrophic components by means of tree-girdling in old boreal spruce forest. Forest Ecology and Management, 257(8), 1764-1767.

Hui, D. F., & Luo, Y. Q. (2004). Evaluation of soil CO2 production and transport in Duke Forest using a process-based modeling approach. Global Biogeochemical Cycles, 18(4).

IPCC, (2014). Climate Change 2014: Mitigation of Climate Change. Contribution of Working Group III to the Fifth Assessment Report of the Intergovernmental Panel on Climate Change [Edenhofer, O., R. et al.]. Cambridge University Press, Cambridge and New York.

Jiang, H., Deng, Q., Zhou, G., Hui, D., Zhang, D., Liu, S., et al. (2013). Responses of soil respiration and its temperature/moisture sensitivity to precipitation in three subtropical forests in southern China. Biogeosciences, 10(6), 3963-3982.

Joseph, J., Kulls, C., Arend, M., Schaub, M., Hagedorn, F., Gessler, A., & Weiler, M. (2019). Application of a laser-based spectrometer for continuous in situ measurements of stable isotopes of soil CO2 in calcareous and acidic soils. Soil, 5(1), 49-62. doi:10.5194/soil-5-49-2019

Kool, D. M., Chung, H. G., Tate, K. R., Ross, D. J., Newton, P. C. D., & Six, J. (2007). Hierarchical saturation of soil carbon pools near a natural CO2 spring. Global Change Biology, 13(6), 1282-1293. doi:10.1111/j.1365-2486.2007.01362.x

Lelieveld, J., Hadjinicolaou, P., Kostopoulou, E., Chenoweth, J., El Maayar, M., Giannakopoulos, C., . . . Xoplaki, E. (2012). Climate change and impacts in the Eastern Mediterranean and the Middle East. Climatic Change, 114(3-4), 667-687. doi:10.1007/s10584-012-0418-4

Kowalski, A. S., Serrano-Ortiz, P., Janssens, I. A., Sanchez-Moral, S., Cuezva, S., Domingo, F., et al. (2008). Can flux tower research neglect geochemical CO2 exchange? Agricultural and Forest Meteorology, 148(6-7), 1045-1054.

Kuzyakov, Y. (2006). Sources of CO2 efflux from soil and review of partitioning methods. [Review]. Soil Biology & Biochemistry, 38(3), 425-448.

Lellei-Kovacs, E., Kovacs-Lang, E., Botta-Dukat, Z., Kalapos, T., Emmett, B., & Beier, C. (2011). Thresholds and interactive effects of soil moisture on the temperature response of soil respiration. European Journal of Soil Biology, 47(4), 247-255.

Levin, I., Naegler, T., Kromer, B., Diehl, M., Francey, R. J., Gomez-Pelaez, A. J., et al. (2010). Observations and modelling of the global distribution and long-term trend of atmospheric (CO2)-C-14 (vol 62, pg 26, 2010). Tellus Series B-Chemical and Physical Meteorology, 62(3), 207-207.

Lin, G. H., Ehleringer, J. R., Rygiewicz, P. T., Johnson, M. G., & Tingey, D. T. (1999). Elevated CO2 and temperature impacts on different components of soil CO2 efflux in Douglas-fir terracosms. Global Change Biology, 5(2), 157-168.

Litton, C. M., Raich, J. W., & Ryan, M. G. (2007). Carbon allocation in forest ecosystems. Global Change Biology, 13(10), 2089-2109.

Lopez-Ballesteros, A., Serrano-Ortiz, P., Kowalski, A. S., Sanchez-Canete, E. P., Scott, R. L., & Domingo, F. (2017). Subterranean ventilation of allochthonous CO2 governs net CO2 exchange in a semiarid Mediterranean grassland. Agricultural and Forest Meteorology, 234, 115-126. doi:10.1016/j.agrformet.2016.12.021

Luyssaert, S., Inglima, I., Jung, M., Richardson, A.D., Reichstein, M., Papale, D., et al. (2007). CO2 balance of boreal, temperate, and tropical forests derived from a global database. Glob. Change Biol. 13, 2509–2537.

Maseyk, K., Grünzweig, J. M., Rotenberg, E., & Yakir, D. (2008a). Respiration acclimation contributes to high carbon-use efficiency in a seasonally dry pine forest. Global Change Biology, 14(7), 1553-1567.

Matteucci M, Gruening C, Ballarin IG, Seufert G, Cescatti A. (2015). Components, drivers and temporal dynamics of ecosystem respiration in a Mediterranean pine forest. Soil Biology & Biochemistry 88: 224–235

Misson, L., Rocheteau, A., Rambal, S., Ourcival, J. M., Limousin, J. M., & Rodriguez, R. (2010). Functional changes in the control of carbon fluxes after 3 years of increased drought in a Mediterranean evergreen forest? Global Change Biology, 16(9), 2461-2475. doi:10.1111/j.1365-2486.2009.02121.x

Pataki, D. E., Ehleringer, J. R., Flanagan, L. B., Yakir, D., Bowling, D. R., Still, C. J., et al. (2003). The application and interpretation of Keeling plots in terrestrial carbon cycle research. Global Biogeochemical Cycles, 17(1).

Peterjohn, W. T., Melillo, J. M., Steudler, P. A., Newkirk, K. M., Bowles, F. P., & Aber, J. D. (1994). RESPONSES OF TRACE GAS FLUXES AND N AVAILABILITY TO EXPERIMENTALLY ELEVATED SOIL

650 TEMPERATURES. Ecological Applications, 4(3), 617-625.
651 Poulter, B., Frank, D., Ciais, P., Myneni, R. B., Andela, N., Bi, J., et al. (2014). Contribution of semi-arid ecosystems
652 to interannual variability of the global carbon cycle. Nature, 509(7502), 600-+.
653 Preisler, Y, Tatarinov, F, Grünzweig, JM, et al. (2019). Mortality versus survival in drought-affected Aleppo pine
654 forest depends on the extent of rock cover and soil stoniness. Funct Ecol.; 00:1–12.
655 Qubaja, R., Grünzweig, J., Rotenberg, E., & Yakir, D. (2019). Evidence for large carbon sink and long residence
656 time in semi-arid forests based on 15-year flux and inventory records. Accepted for Global Change Biology
657 Raich, J. W., & Schlesinger, W. H. (1992). THE GLOBAL CARBON-DIOXIDE FLUX IN SOIL RESPIRATION
658 AND ITS RELATIONSHIP TO VEGETATION AND CLIMATE. Tellus Series B-Chemical and Physical
659 Meteorology, 44(2), 81-99.
660 Ramnarine, R., Wagner-Riddle, C., Dunfield, K. E., & Voroney, R. P. (2012). Contributions of carbonates to soil
661 CO2 emissions. Canadian Journal of Soil Science, 92(4), 599-607. doi:10.4141/cjss2011-025
662 Raz-Yaseef, N., Rotenberg, E., & Yakir, D. (2010). Effects of spatial variations in soil evaporation caused by tree
663 shading on water flux partitioning in a semi-arid pine forest. Agricultural and Forest Meteorology, 150(3), 454-
664 462.
665 Reichstein, M., Rey, A., Freibauer, A., Tenhunen, J., Valentini, R., Banza, J., et al. (2003). Modeling temporal and
666 large-scale spatial variability of soil respiration from soil water availability, temperature and vegetation
667 productivity indices. Global Biogeochemical Cycles, 17(4).
668 Rey, A., Pegoraro, E., Tedeschi, V., De Parri, I., Jarvis, P. G., & Valentini, R. (2002). Annual variation in soil
669 respiration and its components in a coppice oak forest in Central Italy. Global Change Biology, 8(9), 851-866.
670 Roland, M., et al. (2012). Contributions of carbonate weathering to the net ecosystem carbon balance of a
671 mediterranean forest. Thesis submitted to Antwerpen University, Antwerpen, Belgium.
672 Ross, I., Misson, L., Rambal, S., Arneth, A., Scott, R. L., Carrara, A., et al. (2012). How do variations in the temporal
673 distribution of rainfall events affect ecosystem fluxes in seasonally water-limited Northern Hemisphere
674 shrublands and forests? Biogeosciences, 9(3), 1007-1024.
675 Rodeghiero M, Cescatti A. (2005). Main determinants of forest soil respiration along an elevation / temperature
676 gradient in the Italian Alps. Glob Chang Biol 11:1024–1041.
677 Rotenberg, E., & Yakir, D. (2010). Contribution of Semi-Arid Forests to the Climate System. Science, 327(5964),
678 451-454.
679 Schiller, G. (2000), Ecophysiology of Pinus halepensis Mill. and P. brutia Ten, in Ecology, Biogeography and
680 Management of Pinus halepensis and P. brutia Forest Ecosystems in the Mediterranean Basin, edited by G.
681 Ne'eman and L. Trabaud, pp. 51–65, Backhuys, Leiden, Netherlands.
682 Serrano-Ortiz, P., Roland, M., Sanchez-Moral, S., Janssens, I. A., Domingo, F., Godderis, Y., & Kowalski, A. S.
683 (2010). Hidden, abiotic CO2 flows and gaseous reservoirs in the terrestrial carbon cycle: Review and
684 perspectives. Agricultural and Forest Meteorology, 150(3), 321-329. doi:10.1016/j.agrformet.2010.01.002
685 Shachnovich, Y., Berliner, P. R., & Bar, P. (2008). Rainfall interception and spatial distribution of throughfall in a
686 pine forest planted in an arid zone. Journal of Hydrology, 349(1-2), 168-177.
687 Shen, W. J., Jenerette, G. D., Hui, D. F., Phillips, R. P., & Ren, H. (2008). Effects of changing precipitation regimes
688 on dryland soil respiration and C pool dynamics at rainfall event, seasonal and interannual scales. Journal of
689 Geophysical Research-Biogeosciences, 113(G3).
690 Subke, J.-A., Voke, N. R., Leronni, V., Garnett, M. H., & Ineson, P. (2011). Dynamics and pathways of autotrophic
691 and heterotrophic soil CO2 efflux revealed by forest girdling. Journal of Ecology, 99(1), 186-193.
692 Taneva, L., & Gonzalez-Meler, M. A. (2011). Distinct patterns in the diurnal and seasonal variability in four
693 components of soil respiration in a temperate forest under free-air CO2 enrichment. Biogeosciences, 8(10), 3077-
694 3092.
695 Tang, J. W., Baldocchi, D. D., & Xu, L. (2005). Tree photosynthesis modulates soil respiration on a diurnal time
696 scale. Global Change Biology, 11(8), 1298-1304.
697 Tatarinov, F., Rotenberg, E., Maseyk, K., Ogee, J., Klein, T., & Yakir, D. (2016). Resilience to seasonal heat wave
698 episodes in a Mediterranean pine forest. New Phytologist, 210(2), 485-496.
699 Taylor, A. J., Lai, C. T., Hopkins, F. M., Wharton, S., Bible, K., Xu, X. M., et al. (2015). Radiocarbon-Based
700 Partitioning of Soil Respiration in an Old-Growth Coniferous Forest. Ecosystems, 18(3), 459-470.
701 Volcani, A., Karnieli, A., & Svoray, T. (2005). The use of remote sensing and GIS for spatio-temporal analysis of
702 the physiological state of a semi-arid forest with respect to drought years. Forest Ecology and Management,
703 215(1-3), 239-250. doi:10.1016/j.foreco.2005.05.063
704 Wang, X., Liu, L. L., Piao, S. L., Janssens, I. A., Tang, J. W., Liu, W. X., . . . Xu, S. (2014). Soil respiration under
705 climate warming: differential response of heterotrophic and autotrophic respiration. Global Change Biology,

706 20(10), 3229-3237. doi:10.1111/gcb.12620
707 Xu, M., & Qi, Y. (2001). Soil-surface CO2 efflux and its spatial and temporal variations in a young ponderosa pine
708 plantation in northern California. Global Change Biology, 7(6), 667-677.
709 Xu, Z. F., Tang, S. S., Xiong, L., Yang, W. Q., Yin, H. J., Tu, L. H., . . . Tan, B. (2015). Temperature sensitivity of
710 soil respiration in China's forest ecosystems: Patterns and controls. Applied Soil Ecology, 93, 105-110.
711 doi:10.1016/j.apsoil.2015.04.008
712 Yu, S. Q., Chen, Y. Q., Zhao, J., Fu, S. L., Li, Z., Xia, H. P., & Zhou, L. X. (2017). Temperature sensitivity of total
713 soil respiration and its heterotrophic and autotrophic components in six vegetation types of subtropical China.
714 Science of the Total Environment, 607, 160-167. doi:10.1016/j.scitotenv.2017.06.194
715 Zhou, T., Shi, P. J., Hui, D. F., & Luo, Y. Q. (2009). Global pattern of temperature sensitivity of soil heterotrophic
716 respiration (Q(10)) and its implications for carbon-climate feedback. Journal of Geophysical Research-
717 Biogeosciences, 114.